Microbiological Research 170 (2015) 255–262

Contents lists available at ScienceDirect

Microbiological Research

journal homepage: www.elsevier.com/locate/micres

Phenotypic characterization of a novel double knockout PknI/DacB2 from *Mycobacterium tuberculosis*

Srinivasan Kandasamy, Sujatha Narayanan*

Department of Immunology, National Institute for Research in Tuberculosis (NIRT), Mayor V R Ramanathan Road, Chetpet, Chennai 600 031, Tamilnadu, India

ARTICLE INFO

Article history:
Received 23 May 2014
Received in revised form
24 September 2014
Accepted 17 October 2014
Available online 23 October 2014

Keywords:
Mycobacterium tuberculosis
STPK
PBP
Colony morphology
Transmission electron microscope
Biofilm
Cording
MIC

ABSTRACT

Serine/threonine protein kinases play a major role in peptidoglycan biosynthesis in *Mycobacterium tuberculosis*. To explore the mechanism in detail, in the present study, we have constructed a double knockout (DKO) strain lacking pknI and dacB2 in *M. tuberculosis*. Initially, we analyzed the colony morphology and found that the DKO strain showed smoother colony morphology on solid agar and irregular shape in transmission electron microscopy. In addition, the DKO strain exhibits defective biofilm and cord formation. The DKO strain was found to be hypersensitive to cell wall damaging agents such as lysozyme, malachite green, ethidium bromide and to isoniazid, a first line anti-TB drug. In conclusion, our data suggest that both pknI and dacB2 play an important role in the maintenance of colony morphology, cell wall permeability and integrity of *M. tuberculosis*.

1. Introduction

Tuberculosis (TB) is mainly caused by *Mycobacterium tuberculosis* (*M. tuberculosis*), still remains a major cause for increasing global morbidity due to the emergence of drug resistant strains and HIV epidemic (WHO, 2012). *M. tuberculosis* has a capacity to survive in various environmental conditions by modulating cell division and cell wall biosynthesis. The cell wall of mycobacteria consists of three main components, namely mycolic acids (M), arabinogalactan (AG) and peptidoglycan (PG) which are covalently linked to each other and more complex than other bacteria (Jankute et al., 2012). The PG layer is found in nearly all bacteria and responsible for bacterial shape and structural integrity. It has been proved that the PG biosynthesis and cell division processes occur simultaneously in every bacterial cell (Cabeen and Jacobs-Wagner, 2005), but the detailed mechanism behind these processes in mycobacteria has not yet been reported.

Penicillin binding proteins (PBPs) are a group of serine acyl transferases which are involved in the PG biosynthesis, cell wall expansion, septum formation and cell division (Goffin and Ghuysen, 2002). The PBPs can be categorized into high molecular mass (HMM) and low molecular mass (LMM) (Sauvage et al., 2008). Although little is known about the PG biosynthesis regulatory mechanisms in *M. tuberculosis*, there is now an increasing body of evidence indicating that control of PG biosynthesis relies largely on serine/threonine protein kinase (STPK)-dependent mechanisms. It has been reported that pknA, pknB and pknH phosphorylates MurD, GlmU and dacB1,respectively, and regulates the PG biosynthesis in *M. tuberculosis* (Thakur and Chakraborti, 2008; Parikh et al., 2009; Zheng et al., 2007). The pknA, pknB and pknI have been linked to the physiological process of cell wall synthesis/division (Kang et al., 2005; Singh et al., 2006).

The dacB2, a LMM PBP is encoded by an open reading frame (ORF) Rv2911 in *M. tuberculosis* H37Rv. Both dacB2 and pknI are located in the same cluster and are predicted to play a role in PG biosynthesis and cell division (Av-Gay and Everett, 2000). From previous observations, we found that the overexpression of pknI and dacB2 in *M. smegmatis* mc^2 showed similar types of phenotypic alterations like changes in colony morphology and growth rate (Gopalaswamy et al., unpublished data; Bourai et al., 2012). Moreover, the single knockouts ΔpknI and ΔdacB2 exhibits hypervirulent phenotype both *in vitro* and *in vivo* models (Gopalaswamy et al., 2009; Bourai et al., 2012). Furthermore, we found that the

* Corresponding author. Tel.: +044 28369627/+91 9444057490; fax: +91 44 2836 2528.
E-mail address: sujatha.sujatha36@gmail.com (S. Narayanan).

http://dx.doi.org/10.1016/j.micres.2014.10.002
0944-5013/

pknI has a kinase activity and it is dependent on Mn^{2+} for autophosphorylation at serine and threonine residues (Gopalaswamy et al., 2004). It was found that the lysine 41 present in the active site of pknI was essential for kinase activity (Kandasamy et al., 2014). The genomic proximity and similarity of function between pknI and dacB2 has prompted us to study the role of these two genes in *M. tuberculosis*.

In order to gain more insight into the function of pknI and dacB2 in *M. tuberculosis*, a Double Knockout (DKO) strain lacking both the genes was constructed and characterized. The colony morphology of DKO strain was analyzed by transmission electron microscopy (TEM), biofilm and cord formation. The cell wall permeability and integrity of DKO strain was tested by using cell wall damaging agents, TB drugs and β-lactam antibiotics. The findings of this study provide evidence that both pknI and dacB2 play an important role in the maintenance of colony morphology, cell wall permeability and integrity in *M. tuberculosis*.

2. Materials and methods

2.1. Bacterial strains, media, and growth conditions

E. coli strain XL-10 gold (Invitrogen) was used for cloning and *M. smegmatis* mc^2 155 was used for phage propagation. The mycobacterial strains used in this study are listed in Table 1. All the mycobacterial strains were grown in Middlebrook 7H10 solid medium or 7H9 broth (difco) supplemented with 10% oleic acid albumin dextrose catalase supplement (OADC) (BD Biosciences), 0.5% glycerol (Sigma-Aldrich), 0.05% Tween80 (for 7H9 broth alone) in shaking incubator 200 rpm at 37 °C. Kanamycin (20 μg/ml) or hygromycin (50 μg/ml) was added to the 7H9 or 7H10 media to grow *M. tuberculosis* knockout strains harboring antibiotic markers. All the restriction digestion enzymes and other DNA modifying enzymes were purchased from New England Biolabs (NEB), England. The primers used in this study are given in supplementary Table 1. The list of plasmids and phasmids used and generated in this study are listed in Table 1.

Table 1
List of plasmids, phasmids and strains used in this study.

Plasmids/Phasmids	Description	Source
pMV261	*E. coli* – Mycobacterium shuttle vector carrying hsp60 promoter; Kan^r	Stover et al. (1991)
pMV306	*E. coli* – Mycobacterium integrative promoterless vector carrying Kan^r	Stover et al. (1991)
p2911	Suicide recombination delivery vector carrying hygR-sacB disrupting dacB2 in M. tuberculosis H37Rv, HygR	Bourai et al. (2012)
pRG3	pMV306 harboring 1758 bp pknI coding region with its 400 bp upstream region harboring the homologous promoter, Kan^r.	Gopalaswamy et al. (2009)
pKS1	pMV261 harboring 900 bp dacB2 coding region with hsp60 promoter; Kan^r	This study
pKS2	pMV306 harboring dacB2 with hsp60 promoter and pknI gene with homologus promoter	This study
Strains	Description	Reference or source
M. smegmatis mc^2	Wild type strain	Lab stock
H37Rv	*M. tuberculosis* H37Rv wild type strain	Lab stock
ΔpknI	*M. tuberculosis* H37Rv with inactivated pknI	Gopalaswamy et al. (2009)
ΔdacB2	*M. tuberculosis* H37Rv with inactivated dacB2	Bourai et al. (2012)
DKO	*M. tuberculosis* H37Rv with inactivated pknI and dacB2	This study
DKO Comp	DKO strain plus pknI and dacB2	This study
ΔIUM	*M. tuberculosis* H37Rv with unmarked ΔpknI	This study

2.2. Construction, complementation and confirmation of DKO strain

The DKO strain was created by single step homologous recombination using the specialized phage transduction protocol (Bardarov et al., 2002). Using this method, we generated single knockout strains of ΔpknI (Gopalaswamy et al., 2009) and ΔdacB2 (Bourai et al., 2012) and it was used for the construction of DKO strain. Initially, the res-hyg^R-sacB-res cassette was unmarked from ΔpknI by using resolvase phage transduction protocol as described earlier (Bardarov et al., 2002). The unmarked ΔpknI was confirmed by PCR and DNA sequencing. The p2911 phasmid (Table 1) was electroporated into *M. smegmatis* mc^2 for high titer phage preparation. The phages were transduced into unmarked ΔpknI, which was then streaked onto hygromycin impregnated agar plate. The DKO colonies were screened by PCR using primer pairs Hyg^R Fwd and dacB2 RR (Supplementary Table 1).

The DKO colonies were further confirmed by Southern hybridization protocol as described earlier (Bourai et al., 2012). Briefly, genomic DNAs was prepared from wild-type H37Rv and Hyg^R colonies, digested with *XmaI*, separated by 1% agarose gel electrophoresis followed by depurination, denaturation and neutralization of DNA within the agarose gel. DNA was then transferred onto positively charged nylon membranes by capillary transfer using a vacuum blotting apparatus. The 622 base pair in the upstream region of dacB2 was amplified and used for the generation of radio labeled probe. The probe labeling, subsequent pre-hybridization, hybridization and the detection was done as described earlier (Bourai et al., 2012).

For DKO complementation, the DKO strain was transformed with pKS2 plasmid (Table 1) containing two genes (a) the pknI coding region with 400 base pair upstream sequence which might contain the promoter sequence (pRG3) and (b) the dacB2 coding region with the hsp60 promoter (pKS1). The transformation of DKO was performed accordingly to the method of Pavelka and Jacobs, 1999. In brief, pKS2 plasmid was electroporated into the electrocompetent cells of DKO. The cells were then directly plated on 7H10/OADC containing 50 μg/ml of hygromycin plus 30 μg/ml of kanamycin. Then, the DKO complemented strain was confirmed by PCR.

2.3. Colony morphology

The colony morphology was evaluated as described earlier (Russell-Goldman et al., 2008), the mycobacterial cells were grown to mid-log phase in 7H9 medium, washed, resuspended and serially diluted in phosphate-buffered saline (PBS) 0.05% Tween80. Samples of each 10-fold dilution were spotted onto Middlebrook 7H10/OADC and/or 7H11/OADC agar plates (with appropriate antibiotics) and the plates were incubated at 37 °C. The colony images were captured on third and fourth week.

2.4. Transmission electron microscopy examination

Mycobacterial strains were harvested by low speed centrifugation, washed in sterile PBS, and prefixed with a fixation solution containing 2% formaldehyde and 2% glutaraldehyde in 0.1 M sodium cacodylate buffer (pH 7.2) at 4 °C for 1 h. The specimen was immediately cut into small bits of the size 1 mm × 1 mm on a glass slide using a sharp blade. These small specimen bits were transferred back to the fixative and kept immersed for 4 h at 4 °C. The bits were washed with the same buffer thrice, and then it was post-fixed with 0.1% OsO_4 at 8 °C for 2 h. After dehydration,

the specimen bit was embedded in Epon 812 epoxy resin and cut into thin sections using Leica Ultracut R Ultramicrotome. The ultra thin sections were collected on copper Formvar-coated grids and contrasted with 3% solution of uranyl acetate in 70% ethanol for 30 min and then stained with lead citrate at 20 °C for 5 min. After air drying, the sections were examined in JEM 1400 Transmission electron microscope (JEOL) at an accelerating voltage of 80 kV. The micrographs were taken using the Olympus Keenview CCD Camera attached to the microscope.

2.5. Determination of biofilm formation

M. tuberculosis biofilms were generated by modifying published protocols (Ojha et al., 2008) in either 12-well polyvinyl chloride (PVC) plate (Falcon) or petri dishes. Cells from a 7H9 aerated culture ($OD_{600} \sim 1$) were diluted 1:100 (v:v) in Sauton's media, excluding detergent and added to each well and also petri dishes. The plates were wrapped twice with parafilm and incubated at 37 °C for 5 weeks without shaking.

CV staining was carried out by the previously described method (Carter et al., 2003). The medium was removed from wells by pipetting underneath the biofilm at the interface. Biofilms were dried in a bio-safety cabinet and incubated with 500 μl of 1% CV for 10 min. All the wells were washed thrice with distilled water and dried. One mililiter of 95% ethanol was added to each well for 10mins. Then, two fold serial dilutions were read at absorbance at OD_{570nm}.

2.6. Determination of cord formation

For cording analysis, the strains were grown in 7H9 broth without detergent for 3–4 weeks. The culture suspension was spread onto a glass slide, dried and then the slides were stained by using the Ziehl–Neelsen (ZN) and auramine-phenol as described earlier (Selvakumar et al., 2004). The images were observed under a light microscope at 100X using an oil immersion lens in an Olympus binocular microscope (Model CH 30, Olympus, Japan). The fluorescent images were captured at 10× by using an Axio observer microscope.

2.7. Measurement of sensitivity to lysozyme and malachite green

Lysozyme sensitivity was carried out as previously described method (Vandal et al., 2009). Briefly, the mycobacterial strains were incubated at 37 °C for 24 h with 2500 g/ml lysozyme. After incubation, the cells were spotted on 7H10/OADC plates and after 3 weeks the CFU was enumerated.

The malachite green sensitivity was analyzed by two different methods. In the first method, the toxic effect of malachite green was measured by CFU counting (Bianco et al., 2011). Briefly, mid-log phase cultures were washed and adjusted to equal number of cells using McFarlands standards. Equal number of cells was spotted on 7H10/OADC plates with or without 1 mg/l of malachite green. Further, the plates were incubated at 37 °C in the dark and CFUs were counted after 21 days in plates without malachite green and after 40 days in plates containing malachite green.

Secondly, the malachite green decolorization rate was measured as previously described method (Banaei et al., 2009). Briefly, mid-log phase cultures were washed, resuspended in PBS and adjusted to an OD of 0.5. Then, malachite green was added to 4 ml of bacterial cultures at a concentration of 0.1 mg/l. An aliquot of culture was removed every 10 min intervals and the absorbance was measured at 620 nm. Since the malachite green is photooxidation sensitive, the tubes were covered with foil.

2.8. Measurement of sensitivity to sodium dodecyl sulphate

Two methods were used to determine the sensitivity of *M. tuberculosis* cultures to sodium dodecyl sulphate (SDS). Firstly, mid-log phase cultures were washed and adjusted to an equal number of cells using McFarland standards. SDS sensitivity was carried out using 7H10/OADC agar plates containing SDS at 0.1%, 0.01% or 0.001% concentrations as previously described method (Kana et al., 2008).

Secondly, the bacterial viability was tested in the presence of high concentration of SDS as previously described method (Banaei et al., 2009). Briefly, the bacterial cultures was grown to mid-log phase and diluted with growth medium to an OD of 0.05 and incubated with SDS 0.05% in duplicate. An aliquot of samples was removed at 0 h, 1 h and 4 h and plated on 7H10/OADC. The plates were incubated at 37 °C for 3–4 weeks and after incubation the CFUs were enumerated.

2.9. Measurement of sensitivity to ethidium bromide

The ethidium bromide (EtBr) sensitivity to mycobacterial cultures was evaluated as previously described method (Bianco et al., 2011). Briefly, the bacterial cultures were grown to mid-log phase and diluted with growth medium to an OD of 0.05. EtBr was added at a concentration 1 μg/ml and 0.5 μg/ml and grown up to 8 days. The viability of EtBr treated cultures was measured on every day at OD_{600nm}.

2.10. Determination of antibiotic susceptibility

The antibiotic susceptibility test was done using two different methods. They are resazurin microtiter assay (REMA) and antibiotic sensi-disk diffusion method. The detailed protocol is mentioned below.

2.10.1. REMA assay

To determine the minimum inhibitory concentrations (MICs) of mycobacterial strains against anti-TB drugs, REMA was performed as previously described method (Palomino et al., 2002). Briefly, 96 wells flat bottom plate was used to perform REMA. Serial twofold dilutions of each drug in 100 μl of 7H9 medium were prepared directly in 96 well plate at concentrations of 1.0 to 0.001 μg/ml for INH, 2.0 to 0.003 μg/ml for rifampicin, 16 to 0.031 μg/ml for ethambutol, 4 to 0.007 μg/ml for streptomycin, 64 to0.125 μg/ml for kanamycin, 8 to 0.015 μg/ml for ofloxacin and 80 to 0.156 μg/ml for ethionamide. Growth controls containing no antibiotic and sterility controls without inoculation were also included. The mid-log phase bacterial culture turbidity was adjusted to McFarland standard tube no. 1 and then diluted to 1:20 μl and 100 μl was used as inoculum. The plates were covered, and sealed in plastic bags, and incubated at 37 °C in the normal atmosphere. After the incubation period, 30 μl of 0.02% of resazurin solution was added to each well and incubated at 37 °C for 24 h. A color change from blue (oxidized state) to pink (reduced state) indicated the growth of mycobacteria and the MIC was defined as the lowest concentration of each drug that prevented this color change.

2.10.2. Antibiotic disk diffusion assay

Zone of inhibition was measured by disk diffusion method as previously described (Flores et al., 2005). Briefly, *M. tuberculosis* cultures were grown to mid-log phase in 10 ml of 7H9 broth with appropriate antibiotics. Bacterial cells were pelleted, washed twice in 7H9 plain medium to remove antibiotics, and resuspended in 10 ml of 7H9 plain medium. Then, 150 μl of washed culture was streaked on 7H10 agar plates and the antibiotic sensi-disk was placed in the center. The following sensi-discs (Sigma) were

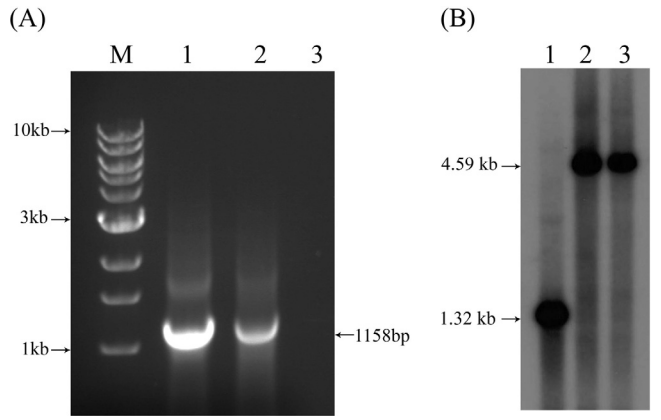

Fig. 1. The genomic DNA of DKO strain and wild-type H37Rv was used as template for PCR. An amplicon of 1158 bp was obtained for DKO strains (lane 1–2) and there was no product obtained for wild-type strain (lane 3). The size of fragment was determined using molecular weight marker (lane M).
DKO strain confirmation by Southern blotting. Genomic DNA of wild-type H37Rv (lane 1) and DKO strain (lane 2–3) was digested with *XmaI* and ran on 1% agarose gel and blotted onto N^+ membrane. The blot was hybridized with labeled left flank. The DKO strain showed a single hybridizing fragment of size 4.59 kb while the wild type H37Rv showed a fragment was around 1.32 kb. The size of fragment was determined using the molecular DNA standards run in parallel.

used in this study, ampicillin (10 mg), amoxicillin/clavulanic acid (20 mg/10 mg), carbenicillin (100 mg), cefixime (5 mg), cefoxitin (30 mg), ceftriaxone (30 mg), imipenem (10 mg) and piperacillin (100 mg). Plates were incubated for 2 weeks and the zone of inhibition was measured by using mm scale.

2.11. Statistical analysis

The significance of the differences between the experimental groups was determined by Student's *t* test using GraphPad prism v.5.0. (** p value <0.001 was said to be significant and *** $p < 0.0001$ was said to be highly significant).

3. Results

3.1. Isolation of DKO and its complemented strains:

In order to explore the role of pknI and dacB2 in *M. tuberculosis* H37Rv, we generated a DKO strain by specialized phage transduction protocol (Bardarov et al., 2002). In the first step, we created an unmarked ΔpknI strain and it was confirmed by PCR (Supplementary Fig. 1A), DNA sequencing (data not shown) and named as ΔIUM strain. Then, the res-hyg^R-sacB-res cassette with ΔdacB2 was inserted by homologous recombination into the ΔIUM strain. As described in Fig. 1A, the DKO strain was first confirmed by PCR. Further, the double deletion was confirmed by Southern blotting, the DKO strain showed a single hybridizing fragment of size 4.59 kb while the wild type H37Rv showed a fragment was around 1.32 kb (Fig. 1B). The DKO strain was complemented using pPKS2 plasmid which is an integration proficient vector and contains pknI and dacB2 gene under the control of homologous and hsp60 promoter, respectively. The success of complementation was confirmed by PCR (Supplementary Fig. 1B) and DNA sequencing (data not shown).

3.2. DKO strain exhibits an alteration in colony morphology

It has been predicted that both pknI and dacB2 have a role in PG biosynthesis. We were interested in the impact that double deletion might have on PG layer, which might be manifested by colony morphology. To test this hypothesis, we analyzed the colony morphology by different methods. Firstly, we observed colony morphology on solid agar and found that the DKO strain showed smoother colony morphology with less ruffling and wrinkled formation when compared to wild type H37Rv strain (Fig. 2A). We observed this phenotypic consistency both on 7H10 and 7H11 agar plates, indicating that the morphological change was not due to nutritional alterations (data not shown). This difference in morphology was reversed by complementation of dacB2 and pknI. The single knockouts did not show any differences in colony morphology (Fig. 2A).

3.3. Electron microscopic examination of DKO strain

The morphological changes in the appearance of *M. tuberculosis* colonies have been reported to be associated with the changes in the cell wall of mycobacteria (Cox et al., 1999). In order to investigate the colony morphology changes in detail, we examined the ultrastructure of single and DKO strains by electron microscopy. As shown in Fig. 2B, the wild type H37Rv strain showed regular rounded multilayered cell envelope, which contains a plasma membrane and a PG layer. However, the DKO strain showed an irregular (zig–zag) colony morphology. Interestingly, the single knockouts ΔpknI and ΔdacB2 presented a normal cell wall structure comparable to the wild type H37Rv (Fig. 2B).

3.4. The DKO strain exhibits defective biofilm and cord formation

Previously it has been proved that, the differences in colony morphology were associated with biofilm formation (Recht and Kolter, 2001). Therefore, we analyzed biofilm formation, the wild type H37Rv was able to span the polystyrene surface and form thickened or developed cords and reticulations characteristic of biofilms. However, the DKO strain showed a thin pellicle and failed to spread on the surface of polystyrene plate (Supplementary Fig. 2A). These results were further confirmed by CV staining, which revealed that the DKO strain was failed to form biofilm (Supplementary Fig. 3A). Quantitative estimation of CV staining also showed a significant reduction of biofilm formation in DKO strain compared to wild type H37Rv strain (Supplementary Fig. 3B). We did not find any differences in biofilm formation for single knockouts and DKO comp.

As seen in Supplementary Fig. 2B, the wild type H37Rv strain formed tight, highly branching serpentine cords. In contrast, DKO strain formed disordered aggregates with many free isolated organisms that lacked obvious cord formation (Supplementary Fig. 2B). Similar to wild type H37Rv, the single knockouts also formed tight highly branching serpentine cords. The DKO complement strain completely recovered the cording defect of DKO strain. This result was further confirmed by auramine phenol staining (Supplementary Fig. 2C).

3.5. DKO strain was highly susceptible to lysozyme and malachite green

We hypothesized that the lack of pknI and dacB2 would have a detrimental effect on PG layer or stability. This hypothesis was evaluated by testing susceptibility of DKO strain to lysozyme. The DKO strain showed significantly increased susceptibility to the enzymatic action of lysozyme when compared to wild type H37Rv or single knockout strains (Fig. 3A). The DKO comp was restored wild type H37Rv phenotype.

Next, we assessed the effect of double deletion on cell wall permeability by malachite green sensitivity. In the presence of malachite green, the DKO strain showed significant reduction in CFU counts when compared to wild type H37Rv strain (Fig. 3B). The sensitivity of DKO strain to malachite green would not be due

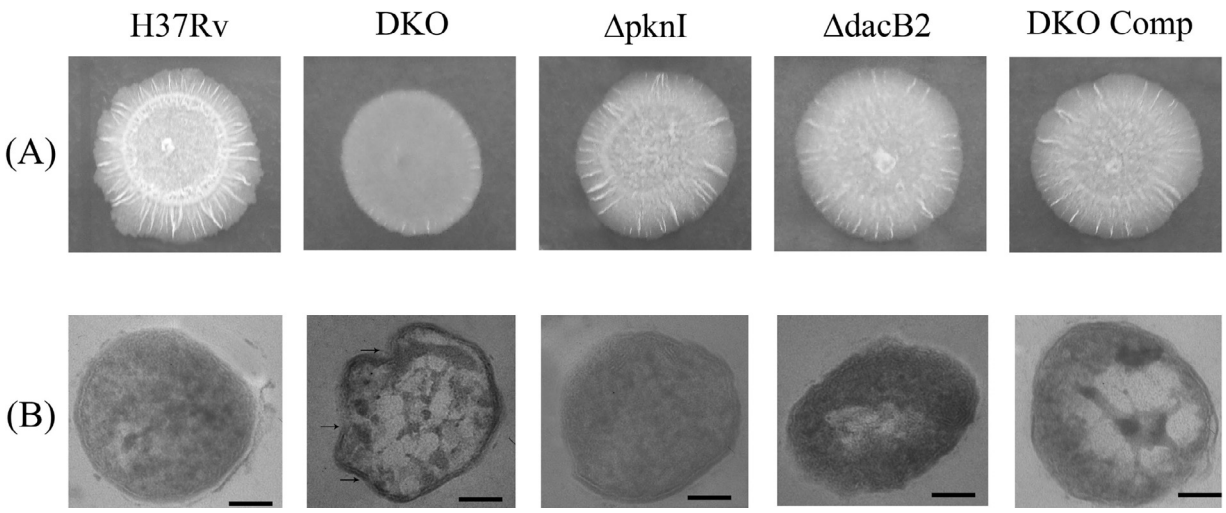

Fig. 2. The DKO strain showed an altered colony morphology and ultrastructure. (A) The DKO strain showed smoother colony morphology in contrast to wild type H37Rv, ΔpknI, ΔdacB2 and DKO Comp strains. The images were taken after incubation at 37 °C for 4 weeks on 7H10 plates. (B) The DKO strain TEM picture showed an irregular shape when compared to wild type H37Rv, ΔpknI, ΔdacB2 and DKO comp strain. The black arrowheads indicate that alterations in cell wall of DKO strain. Scale bar = 50 nm.

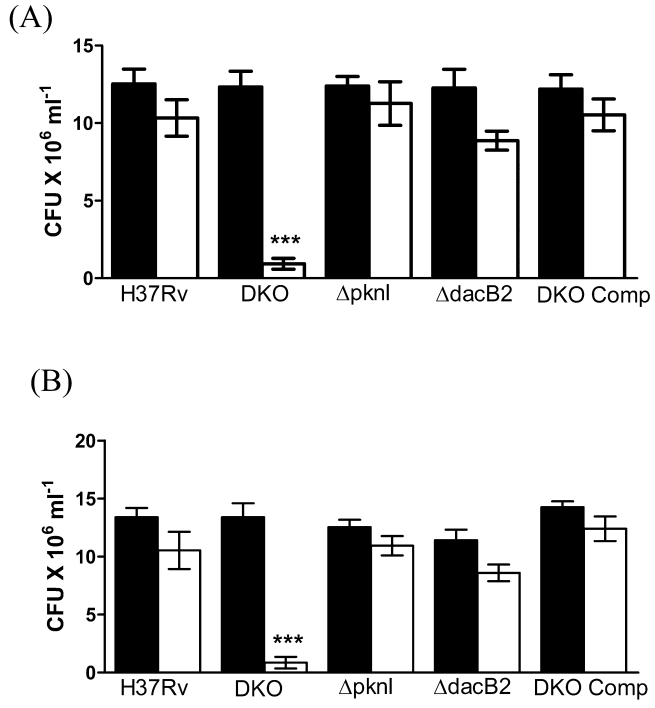

Fig. 3. Measurement of DKO strain sensitivity to lysozyme and malachite green. (A) All mycobacterial strains grown to mid-log phase were diluted to equal growth using McFarlands standard. Then, the mycobacterial strains were incubated without (black bar) or with 2500 μg/ml of lysozyme (white bar) at 37 °C for 24 h. After 3 weeks the CFUs were enumerated. Data are means ± standard deviations from triplicate cultures. Statistically significant differences in survival relative to that of H37Rv are indicated by asterisks (*** $p < 0.0001$). All data are representative of three independent experiments.
(B) All mycobacterial strains grown to mid-log phase were diluted to equal growth using McFarlands standard. 0.1 ml of cells plated on 7H10 plate without (black bar) or with (white bar) 1 mg/l of malachite green. Data are means ± standard deviations from triplicate cultures. Statistically significant differences in survival relative to that of H37Rv are indicated by asterisks (*** $p < 0.0001$). All data are representative of three independent

to the loss of malachite green reducing enzymes, but might be due to alterations in cell wall permeability. To analyze the permeability defect in detail, we assessed malachite green decolorization rate. The DKO strain showed 2.9 fold faster decolorization rate than in PBS whereas the wild type H37Rv showed 1.2 fold only (Supplementary Fig. 4). We did not find any significant difference in malachite green sensitivity for single knockouts. Moreover, we did not observe any significant differences in SDS sensitivity for double and single knockout strains (Supplementary Fig. 5).

Table 2
MIC of mycobacterial strains against anti-TB drugs.

Drug	MIC (μg/ml)				
	Rv	DKO	ΔpknI	ΔdacB2	DKO Comp
Isoniazid	0.06	0.03	0.06	0.06	0.06
Rifampicin	0.01	0.01	0.01	0.01	0.01
Ethambutol	2	2	2	2	2
Ethionamide	0.15	0.15	0.15	0.15	0.15
Kanamycin	4	4	4	4	4
Ofloxacin	1	1	1	1	1
Streptomycin	0.5	0.5	0.5	0.5	0.5

3.6. Sensitivity of DKO strain to EtBr

The TEM studies showed the alterations in the ultrastructure of DKO strain (Fig. 2B). We hypothesized that the pknI and dacB2 double deletion might lead to changes in transport of small molecules across the cell wall by altering the efflux pumping system. To test this hypothesis, we decided to examine the susceptibility of DKO strain to EtBr. We found that the DKO strain showed significant growth reduction in the presence of EtBr when compared to wild type H37Rv strain (Fig. 4). We did not find any significant differences for single knockout strains (Fig. 4).

3.7. Sensitivity of DKO strain to antibiotics

We tested the antibiotic susceptibility of DKO strain to first and second line TB drugs. We found that the DKO strain was twofold more susceptible to INH than wild type H37Rv strain and did not show any difference for rifampicin, ethambutol, ethionamide, kanamycin, ofloxacin and streptomycin (Table 2). The single knockouts of ΔpknI and ΔdacB2 did not show any difference in antibiotic susceptibility to these drugs. Likewise, the DKO comp strain showed a similar profile of drug resistance when compared to wild type H37Rv.

The susceptibility of mycobacterial strains to β-lactam drugs were analyzed by disk diffusion using Sensi-disk. This method has

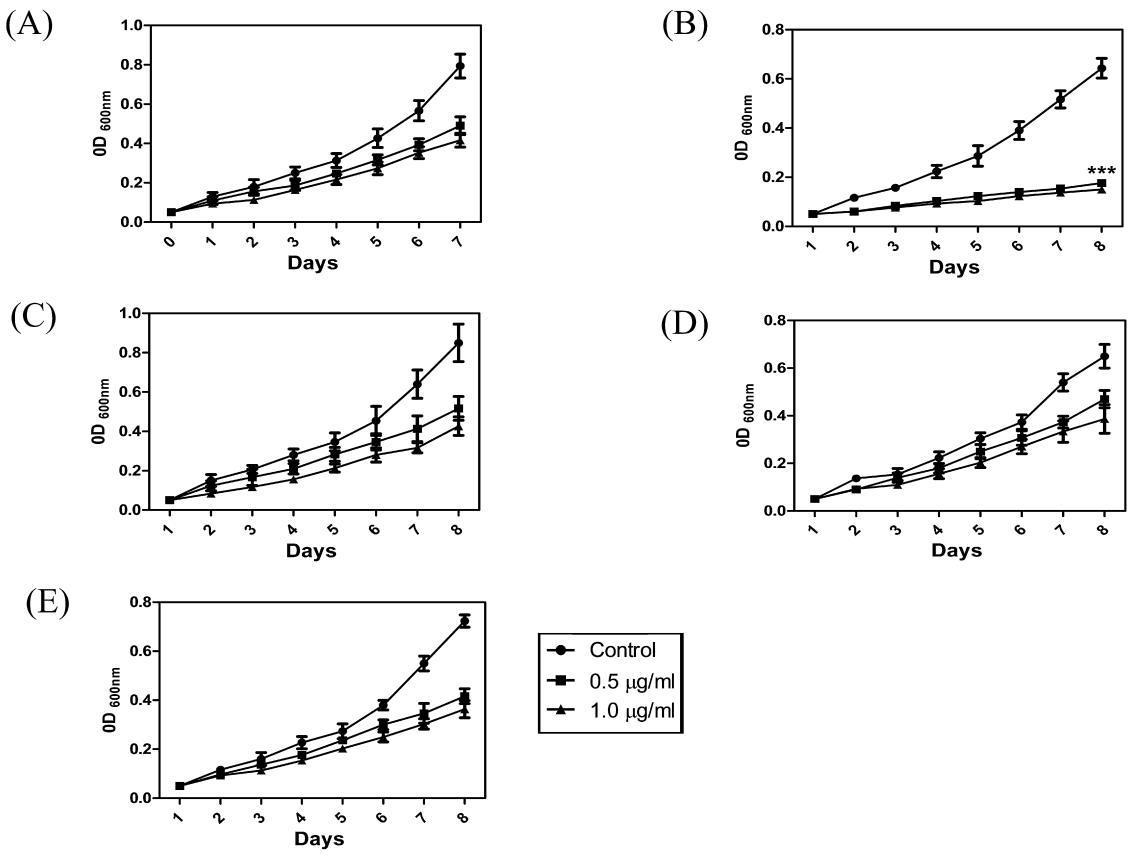

Fig. 4. DKO strain was highly sensitive to EtBr. Bacterial strains were grown to mid-log phase were diluted in 7H9 medium either without or with 1 μg/ml or 0.5 μg/ml of EtBr and growth was determined over time as indicated. Growth curves of (A) H37Rv, (B) DKO (C) ΔpknI, (D) ΔdacB2 and (E) DKO comp strains are representative of three independent experiments. *** denotes $p < 0.0001$ when DKO compared to control. experiments.

been used in the past for susceptibility determinations in slow growing mycobacteria (Flores et al., 2005; Jarboe et al., 1998). We did not find any significant differences for single and DKO strains to β-lactam antibiotics (Supplementary Table. 2).

4. Discussion

To investigate the endogenous role of pknI and dacB2 in mycobacteria, we have successfully generated a ΔpknIΔdacB2 DKO strain and observed phenotypic changes in (a) colony morphology and ultrastructure, (b) biofilm and cord formation and (c) sensitivity to lysozyme, malachite green, EtBr and INH. Based on the earlier report and our studies, we hypothesized that both pknI and dacB2 might play a role in PG biosynthesis (Av-Gay and Everett, 2000; Gopalaswamy et al., 2009; Bourai et al., 2012). In support of our hypothesis, the DKO strain showed colony morphology smooth and irregular shape. It has been proved that the deletion of genes which are involved in the cell wall biosynthesis leads to changes in the colony morphology. In concordance with our results the deletion of kasB, which was involved in the mycolic acid synthesis, caused altered colony morphology and cord formation (Bhatt et al., 2007). Furthermore, the resuscitation promoting factor (Rpf) was reported to share structural similarity with PG degrading enzyme, the double deletion of RpfA/RpfB also caused altered colony morphology (Russell-Goldman et al., 2008). These results suggest that the altered colony morphology of DKO was likely due to changes in the cell wall PG content. Besides, the DKO strain exhibits defective biofilm and cord formation. This clearly shows there could be any alterations in the cell wall profile or changes in the cell wall hydrophobicity and integrity (Rose et al., 2004; Ojha et al., 2005; Makinoshima and Glickman, 2005). Taken together, these results confirm that both pknI and dacB2 play a crucial role in the maintenance of colony morphology, cell wall hydrophobicity and integrity in *M. tuberculosis*.

M. tuberculosis has an impermeable cell envelope and is extremely resistant to lysozyme, which damages the PG layer by hydrolyzing glycosidic bonds in PG or by displacing cell wall autolytic enzymes that normally mediate remodeling during cell division (Keep et al., 2006). The wild type H37Rv strain was resistant to lysozyme up to 2.5 mg/ml but the DKO strain was markedly more susceptible to lysozyme. This finding suggests that the DKO cell envelope is permeable to lysozyme, leading to decreased viability. Similarly, the ΔiipA and ΔexpA knockout strains displayed abnormal colony morphology and increased susceptibility to lysozyme (Gao et al., 2006; Flores et al., 2005). Furthermore, the DKO strain found to be more susceptible to malachite green and EtBr, these might be due to changes in the cell wall permeability and integrity. In the same manner, the lspA and lprG-Rv1410c operon mutants also displayed abnormal colony morphology and showed hypersensitivity to malachite green and EtBr (Banaei et al., 2009; Farrow and Rubin, 2008). We propose that the increased susceptibility of DKO strain to cell wall damaging agents is either directly due to the defects in PG biosynthesis or indirectly due to perturbations of processes that involve the PG or changes in cell wall composition.

The double deletion of pknI and dacB2 led to increased susceptibility of DKO strain to bactericidal drug INH (McDermott, 1959), which inhibits the mycolic acid synthesis pathway (Winder and Collins, 1970; Takayama et al., 1972) required for cell wall synthesis. In contrast, the DKO strain did not alter the susceptibility of other TB drugs, for example rifampicin, which targets RNA polymerase (Karakousis, 2009). To support our results, it has been reported that the ΔMSEG4722 mutant showed altered

colony morphology and increased sensitivity to anti-TB drugs such as rifampicin (Bhatt et al., 2008). These results suggest that the changes in the PG content leads to increased sensitivity of the DKO strain to INH. This result highlights the attractiveness of pknI and dacB2 as an important drug target.

Though, the single knockout strains of ΔpknI and ΔdacB2 did not show differences in any of these phenotypic studies, the DKO comp strain was restored the wild type characteristics. The lack of changes in the single knockouts might be due to various reasons. One possible reason could be that, *M. tuberculosis* posses 11 STPKs (Molle and Kremer, 2010) and 10 PBPs (Sauvage et al., 2008) either one or more of these genes could complement the defective gene functions. However, results in this study suggest that both the pknI and dacB2 are essential to maintain the PG biosynthesis in *M. tuberculosis*. Further studies will be needed to analyze the changes in the cell wall composition to clarify these intriguing observations.

In conclusion, our study suggest that double deletion of pknI and dacB2 in *M. tuberculosis* leads to alterations in the PG layer which were manifested by changes in the colony morphology. These alterations in the PG layer of DKO strain, caused hypersensitivity to various cell wall damaging agents and to INH. Overall, the results obtained in this study clearly demonstrates that both pknI and dacB2 are functionally connected with PG biosynthesis processes associated with maintenance of colony morphology, cell wall permeability, hydrophobicity and integrity in *M. tuberculosis*.

Acknowledgments

Mr. Srinivasan Kandasamy is a recipient of ICMR-SRF fellowship. We thank Dr. Pushba Viswanathan, Cancer Institute for her help in electron microscopic studies. We thank Dr. Radha Madhavan, Professor, Department of Medical Microbiology, SRM University, and for her help in light microscopic studies.

Appendix A. Supplementary data

Supplementary data associated with this article can be found, in the online version, at http://dx.doi.org/10.1016/j.micres.2014.10.002.

References

Av-Gay Y, Everett M. The eukaryotic-like Ser/Thr protein kinases of *Mycobacterium tuberculosis*. Trends Microbiol 2000;8(5):238–44.

Banaei N, Kincaid EZ, Lin SY, Desmond E, Jacobs WR Jr, Ernst JD. Lipoprotein processing is essential for resistance of *Mycobacterium tuberculosis* to malachite green. Antimicrob Agents Chemother 2009;53(9):3799–802.

Bardarov S, Bardarov S Jr, Pavelka MS Jr, Sambandamurthy V, Larsen M, Tufariello J, et al. Specialized transduction: an efficient method for generating marked and unmarked targeted gene disruptions in *Mycobacterium tuberculosis, M. bovis* BCG and *M. smegmatis*. Microbiology 2002;148(Pt 10):3007–17.

Bhatt A, Fujiwara N, Bhatt K, Gurcha SS, Kremer L, Chen B, et al. Deletion of kasB in *Mycobacterium tuberculosis* causes loss of acid-fastness and subclinical latent tuberculosis in immunocompetent mice. Proc Natl Acad Sci USA 2007;104(12):5157–62.

Bhatt A, Brown AK, Singh A, Minnikin DE, Besra GS. Loss of a mycobacterial gene encoding a reductase leads to an altered cell wall containing beta-oxo-mycolic acid analogs and accumulation of ketones. Chem Biol 2008;22(15(9)):930–9.

Bianco MV, Blanco FC, Imperiale B, Forrellad MA, Rocha RV, Klepp LI, et al. Role of P27-P55 operon from *Mycobacterium tuberculosis* in the resistance to toxic compounds. BMC Infect Dis 2011;11:195.

Bourai N, Jacobs WR Jr, Narayanan S. Deletion and overexpression studies on DacB2, a putative low molecular mass penicillin binding protein from *Mycobacterium tuberculosis* H37Rv. Microb Pathog 2012;52(2):109–16.

Cabeen MT, Jacobs-Wagner C. Bacterial cell shape. Nat Rev Microbiol 2005;3(8):601–10.

Carter G, Wu M, Drummond DC, Bermudez LE. Characterization of biofilm formation by clinical isolates of *Mycobacterium avium*. J Med Microbiol 2003;52(Pt 9):747–52.

Cox JS, Chen B, McNeil M, Jacobs WR Jr. Complex lipid determines tissue-specific replication of *Mycobacterium tuberculosis* in mice. Nature 1999;402(6757):79–83.

Farrow MF, Rubin EJ. Function of a mycobacterial major facilitator superfamily pump requires a membrane-associated lipoprotein. J Bacteriol 2008;190(5):1783–91.

Flores AR, Parsons LM, Pavelka MS Jr. Characterization of novel *Mycobacterium tuberculosis* and *Mycobacterium smegmatis* mutants hypersusceptible to β-lactam antibiotics. J Bacteriol 2005;187:1892–900.

Gao LY, Pak M, Kish R, Kajihara K, Brown EJ. A Mycobacterial operon essential for virulence *in vivo* and invasion and intracellular persistence in macrophages. Infect Immun 2006;74(3):1757–67.

Goffin C, Ghuysen JM. Biochemistry and comparative genomics of SxxK superfamily acyltransferases offer a clue to the mycobacterial paradox: presence of penicillin-susceptible target proteins versus lack of efficiency of penicillin as therapeutic agent. Microbiol Mol Biol Rev 2002;66(4):702–38.

Gopalaswamy R, Narayanan PR, Narayanan S. Cloning, overexpression, and characterization of a serine/threonine protein kinase pknI from *Mycobacterium tuberculosis* H37Rv. Protein Expr Purif 2004;36(1):82–9.

Gopalaswamy R, Narayanan S, Chen B, Jacobs WR, Av-Gay Y. The serine/threonine protein kinase PknI controls the growth of *Mycobacterium tuberculosis* upon infection. FEMS Microbiol Lett 2009;295(1):23–9.

Jankute M, Grover S, Rana AK, Besra GS. Arabinogalactan and lipoarabinomannan biosynthesis: structure, biogenesis and their potential as drug targets. Future Microbiol 2012;7(1):129–47.

Jarboe E, Stone BL, Burman WJ, Wallace RJ Jr, Brown BA, Reves RR, et al. Evaluation of a disk diffusion method for determining susceptibility of Mycobacterium avium complex to clarithromycin. Diagn Microbiol Infect Dis 1998;30:197–203.

Kana BD, Gordhan BG, Downing KJ, Sung N, Vostroktunova G, Machowski EE, et al. The resuscitation-promoting factors of *Mycobacterium tuberculosis* are required for virulence and resuscitation from dormancy but are collectively dispensable for growth *in vitro*. Mol Microbiol 2008;67(3):672–84.

Kang CM, Abbott DW, Park ST, Dascher CC, Cantley LC, Husson RN. The *Mycobacterium tuberculosis* serine/threonine kinases PknA and PknB: substrate identification and regulation of cell shape. Genes Dev 2005;19:1692–704.

Kandasamy S, Hassan S, Gopalaswamy R, Narayanan S. Homology modelling, docking, pharmacophore and site directed mutagenesis analysis to identify the critical amino acid residue of PknI from *Mycobacterium tuberculosis*. J Mol Graph Model 2014;52:11–9.

Karakousis PC. Mechanisms of action and resistance of antimycobacterial agents. In: Mayers DL, editor. Antimicrobial drug resistance. New York, NY: Humana Press; 2009. p. 271–91.

Keep NH, Ward JM, Cohen-Gonsaud M, Henderson B. Wake up! Peptidoglycan lysis and bacterial non-growth states. Trends Microbiol 2006;14:271–6.

Makinoshima H, Glickman MS. Regulation of *Mycobacterium tuberculosis* cell envelope composition and virulence by intramembrane proteolysis. Nature 2005;436(7049):406–9.

McDermott W. Inapparent infection: relation of latent and dormant infections to microbial persistence. Public Health Rep 1959;74(6):485–99.

Molle V, Kremer L. Division and cell envelope regulation by Ser/Thr phosphorylation: Mycobacterium shows the way. Mol Microbiol 2010;75(5):1064–77.

Ojha A, Anand M, Bhatt A, Kremer L, Jacobs WR Jr, Hatfull GF. GroEL1: a dedicated chaperone involved in mycolic acid biosynthesis during biofilm formation in mycobacteria. Cell 2005;123(5):861–73.

Ojha AK, Baughn AD, Sambandan D, Hsu T, Trivelli X, Guerardel Y, et al. Growth of *Mycobacterium tuberculosis* biofilms containing free mycolic acids and harbouring drug-tolerant bacteria. Mol Microbiol 2008;69(1):164–74.

Palomino JC, Martin A, Camacho M, Guerra H, Swings J, Portaels F. Resazurin microtiter assay plate: simple and inexpensive method for detection of drug resistance in *Mycobacterium tuberculosis*. Antimicrob Agents Chemother 2002;46(8):2720–2.

Parikh A, Verma SK, Khan S, Prakash B, Nadicoori VK. PknB mediated phosphorylateion of a novel substrate, *N*-acetylglucosamine-1-phosphate uridyltransferase, modulates its acyltransferase activity. J Mol Biol 2009;386(2):451–64.

Pavelka MS Jr, Jacobs WR Jr. Comparison of the construction of unmarked deletion mutations in *Mycobacterium smegmatis, Mycobacterium bovis* bacillus Calmette-Guerin, and *Mycobacterium tuberculosis* H37Rv by allelic exchange. J Bacteriol 1999;181:4780–9.

Recht J, Kolter R. Glycopeptidolipid acetylation affects sliding motility and biofilm formation in *Mycobacterium smegmatis*. J Bacteriol 2001;183(19):5718–24.

Rose L, Kaufmann SH, Daugelat S. Involvement of *Mycobacterium smegmatis* undecaprenyl phosphokinase in biofilm and smegma formation. Microbes Infect 2004;6(11):965–71.

Russell-Goldman E, Xu J, Wang X, Chan J, Tufariello JM. A *Mycobacterium tuberculosis* Rpf double- knockout strain exhibits profound defects in reactivation from chronic tuberculosis and innate immunity phenotypes. Infect Immun 2008;76(9):4269–81.

Sauvage E, Kerff F, Terrak M, Ayala JA, Charlier P. The penicillin-binding proteins: structure and role in peptidoglycan biosynthesis. FEMS Microbiol Rev 2008;32(2):234–58.

Selvakumar N, Sudhamathi S, Duraipandian M, Frieden TR, Narayanan PR. Reduced detection by Ziehl–Neelsen method of acid-fast bacilli in sputum samples preserved in cetylpyridinium chloride solution. Int J Tuberc Lung Dis 2004;8(2):248–52.

Singh A, Singh Y, Pine R, Shi L, Chandra R, Drlica K. Protein kinase I of *Mycobacterium tuberculosis*: cellular localization and expression during infection of macrophage-like cells. Tuberculosis (Edinb) 2006;86:28–33.

Stover CK, de la Cruz VF, Fuerst TR, Burlein JE, Benson LA, Bennett LT, et al. New use of BCG for recombinant vaccines. Nature 1991;351(6326):456–60.

Takayama K, Wang L, David HL. Effect of isoniazid on the in vivo mycolic acid synthesis, cell growth, and viability of *Mycobacterium tuberculosis*. Antimicrob Agents Chemother 1972;2(1):29–35.

Thakur M, Chakraborti PK. Ability of PknA, a mycobacterial eukaryotic type serine/threonine kinase, to transphosphorylate MurD, a ligase involved in the process of peptidoglycan biosynthesis. Biochem J 2008;415(1): 27–33.

Vandal OH, Roberts JA, Odaira T, Schnappinger D, Nathan CF, Ehrt S. Acid-susceptible mutants of *Mycobacterium tuberculosis* share hypersusceptibility to cell wall and oxidative stress and to the host environment. J Bacteriol 2009;191(2): 625–31.

WHO. Global tuberculosis report 2012. Geneva, Switzerland: World Health Organization; 2012.

Winder FG, Collins PB. Inhibition by isoniazid of synthesis of mycolic acids in *Mycobacterium tuberculosis*. J Gen Microbiol 1970;63:41–8.

Zheng X, Papavinasasundaram KG, Av-Gay Y. Novel substrates of *Mycobacterium tuberculosis* PknH Ser/Thr kinase. Biochem Biophys Res Commun 2007;355(1):162–8.